

2006

# Numerical Modelling Of Mining Induced Subsidence

W. Keilich

*University of Wollongong*

Ross W. Seedsman

*University of Wollongong, seedsman@uow.edu.au*

N. Aziz

*University of Wollongong, naj@uow.edu.au*

---

## Publication Details

This conference paper was originally published as Keilich, W, Seedsman, R and Aziz, NH, Numerical Modelling Of Mining Induced Subsidence, in Aziz, N (ed), Coal 2006: Coal Operators' Conference, University of Wollongong & the Australasian Institute of Mining and Metallurgy, 2006, 313-326.

---

# NUMERICAL MODELLING OF MINING INDUCED SUBSIDENCE

Walter Keilich<sup>1</sup>, Ross Seedsman<sup>2</sup>, and Naj Aziz<sup>1</sup>

**ABSTRACT:** A methodology of subsidence prediction using the Distinct Element code UDEC has been developed as an alternative for subsidence modelling in the Southern Coalfield, New South Wales, Australia. The models have been validated by comparison with empirical results and observed caving behaviour. At this stage, modelling capability is limited to flat lying terrain. It is planned to apply the methodology to areas of high topographical relief to investigate the mechanics of valley closure.

## INTRODUCTION

Ground subsidence due to mining has been the subject of intensive research for several decades, and it remains to be an important topic confronting the mining industry today. In the Southern Coalfield of NSW, Australia, there is particular concern about subsidence impacts on incised river valleys – valley closure, upsidence, and the resulting localised loss of surface water under low flow conditions. Most of the reported cases have occurred when the river valley is directly undermined. However, there are a number of cases where closure and upsidence is reported above unmined coal. These latter events are especially significant as they influence decisions regarding stand-off distances and hence mine layouts and reserve recovery.

The deformations of the valleys indicate the onset of locally compressive stress conditions. Compressive conditions are anticipated when the surface deforms in a sagging mode, for example directly above the longwall extraction: they are not expected when the surface deforms in a hogging mode. To date, explanations for valley closure under the hogging mode have considered undefined compressive stress redistributions in the horizontal plane, or block translations from the sagging mode. This research is investigating the possibilities of the block translation model.

Subsidence prediction in Australia is currently limited to empirical and numerical techniques. The empirical techniques are suitable for flat lying or gently sloping areas but are unsuitable for areas of large topographical relief. From the available numerical techniques, FLAC has been commonly used for assessing the impacts of longwall mining on river valleys. FLAC has limited application as the code is not capable of modelling discontinuous rock masses effectively.

In this project, a methodology of subsidence prediction using the Distinct Element code UDEC is being developed as an alternative for subsidence modelling in the Southern Coalfield. The UDEC models have been validated by comparison with empirical results and comparison of observed caving behaviour. The expected outcomes will include a reliable subsidence prediction tool capable of simulating ground deformations and sub surface movements in flat terrain and river valleys, and a more complete understanding of valley closure. This paper will present work completed to date.

## SUBSIDENCE IN THE SOUTHERN COALFIELD

During longwall mining, a large void in the coal seam is produced and this disturbs the equilibrium conditions of the surrounding rock strata, which bends downward while the floor heaves. When the goaf reaches a sufficient size, the roof strata will fail and cave. Seedsman (2004) reports that caving does not necessarily occur vertically above the extracted coal panel, but in many cases, caving is defined by a goaf angle that trends over the goaf. This angle is most likely a function of the bedding structure of the roof and the orientation of the goaf with respect to sub vertical jointing.

---

<sup>1</sup> Faculty of Engineering, University of Wollongong

<sup>2</sup> Visiting Fellow, University Of Wollongong

In the Newcastle Coalfield the average goaf angle is  $12^\circ$  with a standard deviation of  $8^\circ$ . Numerical modelling by the CSIRO (1999) of the caving in the Southern Coalfield appears to support a goaf angle value of  $12^\circ$ . Further numerical modelling by Gale (2005) in an unspecified coalfield also supports this value. Caving will cease when the goaf angle encounters a stratigraphic unit strong enough to bridge what is now the effective span. This concept is illustrated in Figure 1. The goaf and overburden strata will then compact over time and become stabilised.

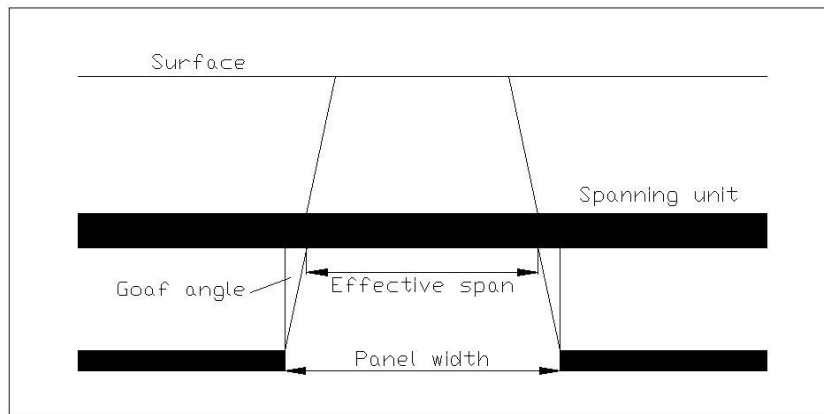


Fig. 1 - Relationship between panel width, goaf angle and effective span

The caving of the roof strata as previously described, gives rise to several zones within the overburden strata. The number of zones varies in the literature with Kratzsch (1983) describing six zones, Peng (1992) describing four zones, and Kapp (1984) describing three zones. These zones are not distinct but there is a gradual transition from one to another. Seedsman (2004) reported on the existence of a massive unit in the strata of the Newcastle Coalfield and presented an alternative way of predicting subsidence based on the Voussior Beam analogue. For this method to be applied, it is assumed that the massive unit remains elastic and all goafing takes place underneath the massive unit. Therefore the developed subsidence is a function of the deflection of the massive unit, provided the massive unit remains elastic and does not fail. Unfortunately, the amount of information on the caving characteristics in the Southern Coalfield is somewhat limited. Microseismic results from an Australian Coal Association Research Program (ACARP) project (CSIRO, 1999) provided some useful information on the caving behaviour at Appin Colliery, which is located in the Southern Coalfield. The longwall panel that was monitored was 200 m wide and extracted the 2.3 m thick Bulli Seam at a depth of about 500 m. The monitoring included the installation of 17 triaxial geophones and nine geophones in a borehole drilled from the surface to the Bulli Seam and two perpendicular surface strings of four geophones each. The period of monitoring was approximately four months, during which there was 700 m of face retreat. From the monitoring it was seen that the majority of fracturing extended approximately 50 m to 70 m above the Bulli Seam with no fracturing exceeding approximately 290 m, and to a depth of 80 m to 90 m into the floor. Figure 2 illustrates the microseismic events in a cross section of the monitored longwall.

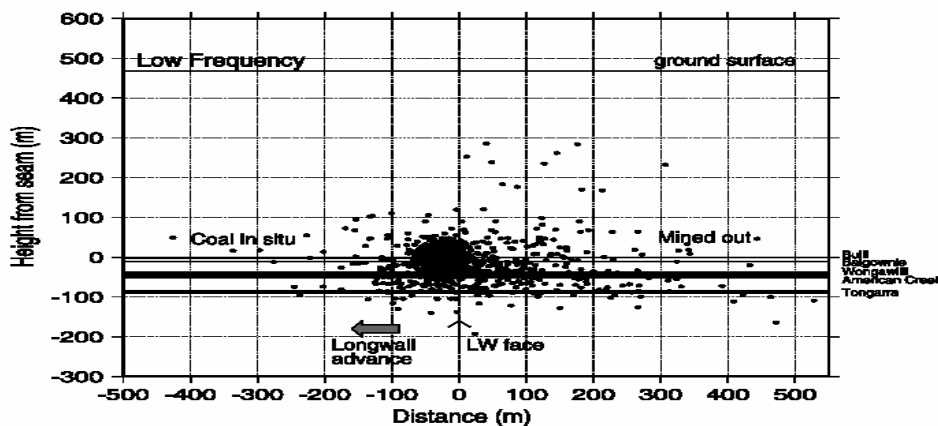


Fig. 2 - Cross section of longwall with microseismic event location (CSIRO, 1999)

An analysis of the stratigraphic details in the subsidence handbook by Holla and Barclay (2000) shows that the Bulgo Sandstone is the most massive unit in the stratigraphy of the Southern Coalfield, with a thickness ranging from approximately 90 m to 200 m, and located at a distance between 90 m and 120 m above the Bulli Seam at Appin Colliery. It is also the strongest of the larger upper units as indicated by a geotechnical characterization (MacGregor and Conquest, 2005). If the position of the Bulgo Sandstone were overlain onto Figure 2, it would be seen that the majority of the fracturing in the goaf is contained by the Bulgo Sandstone. This would seem to suggest that the Bulgo Sandstone is acting as the massive spanning unit, therefore all potential subsidence development can be theoretically derived from a voussoir analysis of the Bulgo Sandstone.

### VALLEY CLOSURE

ACARP (2002) contains a comprehensive literature review on valley bulging, along with an empirical method to predict valley closure, upside, compressive strain and regional horizontal movement for river valleys that have been undermined. It is proposed that during the formation of a river valley, the horizontal stresses in the valley sides redistribute to the valley base, causing an increase in horizontal stress. Bulging of the valley base is a result of this stress redistribution and is a natural phenomenon. When a river valley is undermined, the horizontal stresses are redistributed from the cave zone to the surface. This results in a further increase of the horizontal stress in the valley base. If the elevated horizontal stress exceeds rock strength, the valley base will fail in compression and buckle up-wards or over-ride adjacent stratum. Failure of the valley base continues downward until equilibrium is achieved. This failure of the strata in the base of the valley allows some relaxation of the sides of the valley to occur, causing closure of the valley sides.

For a river valley that is directly undermined by a longwall, the above-mentioned explanation is valid. Results from the empirical study (ACARP, 2002) show that valley closure occurs well outside the goaf edge, up to a longitudinal distance of 1500 m from the end of the longwall. It would be expected that a valley in the convex part of the subsidence profile would open up, not close as seen by the empirical results. Whether this valley closure is driven by the magnitude of horizontal stress or the magnitude of the tilt in the subsidence profile is uncertain and is anticipated to be clarified by numerical modelling.

### EMPIRICAL PREDICTIONS

The method devised by the New South Wales Department of Primary Industries has been in existence since 1985 and is available as a handbook (Holla and Barclay, 2000). Since then, the method has been refined with the addition of subsidence data, and a discussion on the effects of mining induced subsidence on public utilities, dwellings and water bodies. Whilst not accounted for in the prediction technique, there is also a discussion on the major factors modifying the theoretical subsidence behaviour such as faults, dykes, and gullies. Several case studies were also presented to illustrate these factors in action.

The subsidence data and resulting graphs in this method were obtained from collieries in the area between the Illawarra Escarpment and the Burraborang Valley. This data was collected over a period of thirty years. The majority of the mines included in the analyses were mining the Bulli seam except in two cases for which the workings were in the Wongawilli seam. The predominant method of mining was by longwall mining, although some pillar extraction data has been included. The relationship between  $S_{\max}/T$  and  $W/H$  for single panels is illustrated in Figure 3.

It can be seen from Figure 3 that the lower curve represents the relationship between the width to cover depth ( $W/H$ ) and subsidence factor ( $S_{\max}/T$ ) for longwall extraction, where  $S_{\max}$  is the maximum developed subsidence and  $T$  is the extracted thickness. It can also be seen from Figure 3 that the largest longwall  $W/H$  ratio still falls into the sub-critical category ( $W/H < 1.4$ ). This is a result of the deep mining conditions in the Southern Coalfield, and although data exists for  $W/H$  ratios between 0.5 and 0.9, the resulting scatter suggests that subsidence prediction would be more accurate for  $W/H$  ratios less than 0.5.

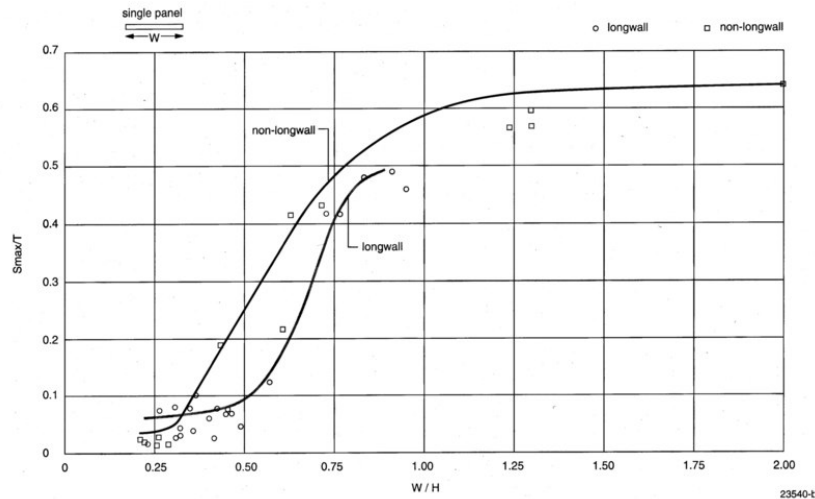


Fig. 3 - Relationship between  $S_{\max}/T$  and  $W/H$  for single longwall panels (Holla and Barclay, 2000)

### NUMERICAL MODELLING STRATEGY

The approach used in the numerical modelling was to try and replicate the trends in Figure 3 before extending the numerical modelling to undermined river valleys in an effort to understand the mechanisms behind valley closure. Holla and Barclay (2000) contain a list of mines and extraction details, from which the ground movement data were collected and the subsidence curves derived (single panel only). The majority of the mines extracted the Bulli Seam using the longwall method of mining. The data that was derived from pillar extraction and Wongawilli Seam extraction was excluded from the modelling. It should be noted that the extraction details are approximate figures only.

Holla and Barclay (2000) also contain the thickness of the stratigraphic units in the overburden, grouped according to colliery. This was used for the derivation of the thickness of rock units above the Bulli seam for different mines. Excluding mines that utilise pillar extraction, extract the Wongawilli Seam, it was concluded that a minimum of three models can be created from the available data (Table 1).

Table 1 - Basic details of models

Model Name	Individual Panel Width $W$ (m)	Cover Depth $H$ (m)	Extracted Thickness (m)	$W/H$
Model 1	105	413	2.7	0.25
Model 2	158	450	2.5	0.35
Model 3	160	288	3.0	0.56

It must be noted that although 18 potential models can be created with the available data, three models was considered sufficient to cover the range of  $W/H$  ratios represented in the single panel subsidence curve in Figure 3. At the time of writing, another model with a  $W/H$  ratio of 0.81 was running but early indications suggest a model this large is impractical to run, with the current run time of this model exceeding two weeks.

### Model Geometry

Symmetry has been utilised to halve the size of the models needed, with the right hand side of the model representing the centreline of the panel. Each model has the left hand boundary fixed at five times the excavation width, as indicated by the UDEC user's manual (Itasca, 2000), or the predicted range of ground movement as indicated by the 29° angle of draw (Holla and Barclay, 2000), or whichever is the greater value. The stratigraphic thickness for each rock unit in the Southern Coalfield is given in Table 2 and the finalised dimensions for each model are given in Table 3. Bedding planes were assumed as horizontal and vertical joints were placed with a 90° dip and offset to form a brickwork style pattern.

Table 2 - Thickness of stratigraphic units for each model, in descending order

		Model Name		
		1	2	3
Stratigraphic Unit Thickness (m)	Hawkesbury Sandstone	88	153	78
	Newport Formation	20	13	7
	Bald Hill Claystone	34	23	12
	Bulgo Sandstone	145	156	92
	Stanwell Park Claystone	40	23	11
	Scarborough Sandstone	50	32	36
	Wombarra Shale	16	29	29
	Coal Cliff Sandstone	20	21	23
	Bulli Seam	2.7	2.5	3
	Loddon Sandstone	8	8	8
	Balgownie Seam	1	1	1
	Lawrence Sandstone	4	4	4
	Cape Horn Seam	2	2	2
	UN2*	6	6	6
	Hargraves Coal Member	0.1	0.1	0.1
	UN3*	10	10	10
	Wongawilli Seam	10	10	10
	Kembla Sandstone	3	3	3
	Lower Coal Measures	50	50	50
	Total Depth	509.8	546.6	385.1

\*UN-NAMED MEMBER

Table 3 - Finalised width and depth for each model

Model Name	Total Model Width (m)	Total Model Depth (m)
Model 1	315	509.8
Model 2	474	546.6
Model 3	480	385.1

### Material Properties

A great deal of information has been published on the material properties of the stratigraphic units above and including the Bulgo Sandstone by Pells (1993). Most of this data is derived from civil engineering works in and around Sydney, not specifically the Southern Coalfield. Most recently, a drilling program has been completed which contains the geotechnical characterisation of several boreholes that were drilled over Appin and Westcliff collieries (MacGregor and Conquest, 2005). As a result of this geotechnical characterisation and a survey of the literature (CSIRO, 2002; Williams and Gray, 1980; and McNally, 1996) a complete set of material properties have been derived (Table 4). The material properties that have been derived from laboratory testing have been used directly in the models without calibration or modification.

Table 4 - Selected material properties for stratigraphic units

	E (GPa)	$\nu$	c (MPa)	$\phi$ (°)	$\sigma_T$ (MPa)
Hawkesbury Sandstone	13.99	0.29	9.70	37.25	3.58
Newport Formation	11.65	0.25	8.85	35.00	3.40
Bald Hill Claystone	10.37	0.46	10.60	27.80	2.90
Bulgo Sandstone	18.00	0.23	17.72	35.40	6.55
Stanwell Park Claystone	19.20	0.26	14.57	27.80	4.83
Scarborough Sandstone	20.57	0.23	13.25	40.35	7.18
Wombarra Shale	17.00	0.37	14.51	27.80	4.81
Coal Cliff Sandstone	23.78	0.22	19.40	33.30	7.87
Bulli Seam	2.80	0.30	6.37	25.00	0.84

Table 4 - Selected material properties for stratigraphic units (continued)

	<b>E (GPa)</b>	<b><math>\nu</math></b>	<b>c (MPa)</b>	<b><math>\phi</math> (°)</b>	<b><math>\sigma_T</math> (MPa)</b>
<b>Loddon Sandstone</b>	15.07	0.33	17.10	28.90	5.65
<b>Balgownie Seam</b>	2.80	0.30	6.37	25.00	0.84
<b>Lawrence Sandstone</b>	15.07	0.33	17.10	28.90	5.65
<b>Cape Horn Seam</b>	2.00	0.30	2.87	25.00	0.70
<b>UN2</b>	13.48	0.25	19.89	28.90	6.74
<b>Hargraves Coal Member</b>	2.80	0.30	6.37	25.00	0.84
<b>UN3</b>	13.00	0.25	19.18	28.90	6.50
<b>Wongawilli Seam</b>	2.00	0.30	2.87	25.00	0.70
<b>Kembla Sandstone</b>	18.15	0.28	18.02	28.90	6.11
<b>Lower Coal Measures</b>	9.37	0.29	12.20	27.17	3.75

Where,

- E = Young's Modulus  
 $\nu$  = Poisson's Ratio  
c = Cohesion  
 $\phi$  = Friction Angle  
 $\sigma_T$  = Tensile Strength

#### Bedding Planes and Properties

Bedding, stratification or layering is one of the most fundamental and diagnostic features of sedimentary rocks. In numerical modelling, it is important to correctly distinguish what constitutes bedding planes and intrabed structures as bedding planes are the major source of shear and slip in a discontinuous rock mass.

Bedding is due to vertical differences in lithology, grain size, grain shape, packing or orientation. Generally, bedding is layering within beds on a scale of about 1 or 2 cm, and lamination is layering within beds on a scale of 1 or 2 mm (Tucker, 2003; and Selley, 2000). Limited information exists about bedding planes in the Southern Coalfield. Most of the information has been derived from civil engineering works and visual examination of outcrops along the coast by Ghobadi (1994). It is also recognised that strata thickness and bedding plane thickness will vary from site to site, so it would be advantageous to derive the required information from a complete geotechnical investigation at one site, if possible.

The drill cores that were obtained for the geotechnical characterisation (MacGregor and Conquest, 2005) were logged for discontinuities, but unfortunately bedding planes or drilling induced fractures were not specifically identified. The authors were allowed access to the logs and laboratory reports. Neutron and gamma logging was also performed on holes. A site visit was conducted by the authors and a visual examination of the core, along with a comparison of the logs was carried out for the Bulgo Sandstone. It was found that there was a good correlation between major bedding planes and partings identified in the core and the corresponding logs. When compared to data provided by Pells (1993) and Ghobadi (1994), there was good agreement apart from the Newport Formation and Bald Hill Claystone. In these instances, it was decided to use the values provided by Pells (1993). The bedding plane spacings used in the models are summarised in Table 5.

Table 5 - Bedding plane spacing

<b>Rock Unit</b>	<b>Bedding Plane Spacing (m)</b>
Hawkesbury Sandstone	9
Newport Formation	1
Bald Hill Claystone	0.3
Bulgo Sandstone	9
Stanwell Park Claystone	3
Scarborough Sandstone	4
Wombarra Claystone	3
Coal Cliff Sandstone	3

Information on specific bedding plane properties are scarce and if the discontinuities are not directly laboratory tested, estimates or values from field studies have to be used. Derivation of the joint and normal and shear stiffness was done in accordance to the procedures described by Itasca (2000). It seems that the shear stiffness can be approximated as one-tenth of the normal stiffness. This approach has been used by Itasca (2000), and has been used by Coulthard (1995) and Badelow et al (2005). The derived joint normal and shear stiffness used for each rock unit is shown in Table 6.

The joint and bedding plane strength parameters have been derived from Chan, Kotze and Stone (2005), and Barton (1976) has been used to calculate cohesion based on the JRC and JCS values given by Chan, Kotze and Stone (2005). The bedding plane properties used in the models can be seen in Table 7.

### Vertical Joints and Properties

Very little data exists on the vertical joint spacing in rock units in the Southern Coalfield, and even where geotechnical characterisations have been completed; vertical joint spacing simply cannot be assessed from HQ cores.

Price (1966) reports on work done in Wyoming, USA, which suggests for a given lithological type, the concentration of joints is inversely related to the thickness of the bed. Examples were given for dolomite where joints in a 10 ft. thick bed occurred at every 10 ft.; and joints in a 1 ft. thick bed occurred every 1 ft. Similar results were also reported for sandstone and limestone. The mechanism proposed by Price (1966) assumed that the cohesion between adjacent beds is non-existent and that friction angle; normal stress and tensile strength are all constant. It was suggested that while these parameters will change in reality, these factors cause only second-order variations in the relationship between joint frequency and bed thickness. A comprehensive review of the Price model was performed by Mandl (2005). In addition, this review also included Hobbs' model, which is a more complex model that takes into account the elastic modulus and bedding plane cohesion of adjacent beds. Both models predict a joint spacing that scales with bed thickness.

**Table 6 - Joint normal and shear stiffness**

Rock Unit	Normal Stiffness (GPa/m)	Shear Stiffness (GPa/m)
Hawkesbury Sandstone	21	2.1
Newport Formation	140	14
Bald Hill Claystone	204	20.4
Bulgo Sandstone	26	2.6
Stanwell Park Claystone	78	7.8
Scarborough Sandstone	76	7.6
Wombarra Claystone	115	11.5
Coal Cliff Sandstone	108	10.8

Ghobadi (1994) reports that the vertical joint spacing in the Hawkesbury Sandstone is observed to be 2-5 m, the Scarborough Sandstone 1-4 m, the Bulgo Sandstone 0.5-1.5 m, the Stanwell Park Claystone 0.1-0.5 m, and the Wombarra Claystone 0.2-0.6 m apart. It was noted that many of the joints on the escarpment and coastline are filled with calcite and/or clay. These values are not in good agreement with the Price joint model.

**Table 7 - Bedding plane properties**

Property	Bedding Plane
Friction Angle (°)	28
Residual Friction Angle (°)	15
JCS	4
JRC	5
Cohesion (MPa)	0.7
Residual Cohesion (MPa)	0
Dilation Angle (°)	0
Tensile Strength (MPa)	0



Pells (1993) reports that the vertical joint spacing in the Hawkesbury Sandstone is 7-15 m in the Southern catchment area, the Newport Formation 1-3 m, Bald Hill Claystone 1 m, and the Bulgo Sandstone 2-13 m. These values are in good agreement with the Price joint model, therefore it was assumed that vertical joint spacing is equal to bed thickness and this assumption was used in the numerical models. Vertical joint properties have been estimated in the same manner as for bedding planes. The vertical joint properties are shown in Table 8.

**Table 8 - Vertical joint properties**

Property	Vertical Joint
Friction Angle (°)	28
Residual Friction Angle (°)	15
JCS	2
JRC	8
Cohesion (MPa)	1
Residual Cohesion (MPa)	0
Dilation Angle (°)	0
Tensile Strength (MPa)	0

### In-Situ Stress

A thorough review of regional and local in-situ stress has been compiled by the CSIRO (2002) for their numerical modelling. From 206 measurements across the Sydney Basin, the ratio of horizontal stress to vertical stress was found to be in the range of 1.5-2.0. For the numerical models, a horizontal to vertical stress ratio of two was implemented.

### Mesh Generation

The mesh employed was relatively simple. Each block was subdivided into four constant strain zones. It was noted by Coulthard (1995) that this may result in a unit of large blocks excessively stiffer than a unit of smaller blocks. This is particularly noticeable where the larger unit overlies the smaller one. If this occurs in the models, the mesh density will be increased in the areas of interest.

### Constitutive Models

The constitutive model employed is the Mohr-Coulomb model. The constitutive model used for the joints is the Mohr-Coulomb residual strength model. This joint model has the capability to reduce or increase friction, cohesion, dilation and tensile strength.

## RESULTS

Three models (Models 1, 2 and 3) had been run and analysed. A fourth model representing a W/H ratio of 0.81 was running at the time of writing but its excessive run times may rule it out in any further analysis. The results have been analysed and plots produced for:

- $S_{\max}/T$  (subsidence factor),
- $S_{\text{goaf}}/S_{\max}$ ,
- K1 (maximum tensile strain constant),
- K2 (maximum compressive strain constant),
- K3 (maximum tilt constant), and
- D/H (position of inflection point relative to goaf).

Strain and tilt are defined by the equation (Holla and Barclay, 2000):

$$+E_{\max}, -E_{\max}, G_{\max} = 1000 \times K \times \frac{S_{\max}}{H}$$

Where,

$+ E_{\max}$	=	Max tensile strain
$- E_{\max}$	=	Max compressive strain
$G_{\max}$	=	Max tilt
K	=	Constant
H	=	Depth of cover

Horizontal strain is the change in length per unit of the original horizontal length of ground surface. Tensile strains occur in the trough margin and over the goaf edges. Compressive strains occur above the extracted area. Holla and Barclay (2000) noted that maximum tensile strains are generally not larger than 1 mm/m and maximum compressive strains 3 mm/m, excluding topographical extremes.

Tilt of the ground surface between two points is found by dividing the difference in subsidence at the two points by the distance between them. Maximum tilt occurs at the point of inflection where the subsidence is roughly equal to one half of  $S_{\max}$ .

The point of inflection is the location where tensile strains become positive and vice versa. It has been found by Holla and Barclay (2000) that the inflection point lies inside the goaf for W/H ratios greater than 0.5.

The respective maximum values were readily picked from the model outputs. The strain profiles for Models 2 and 3 contained anomalies where strain turned compressive in two sections of the profile above unmined coal. However, the magnitude of the strains was extremely low and this behaviour has been ascribed to the modelling technique.

Block failure and the formation of the caved zone can be seen in Figure 4. Block failure trends inward over the goaf at an angle of approximately  $12^\circ$  to  $15^\circ$ . This is in good agreement with the CSIRO (1999) and Gale (2005). The caved zone also stops abruptly at the base of the Bulgo Sandstone; this is in general agreement with the microseismic monitoring (CSIRO, 1999).

Slip occurs on every bedding plane up to the surface, and vertical joints open up in the caved zone and also along the surface, outside the goaf edge.

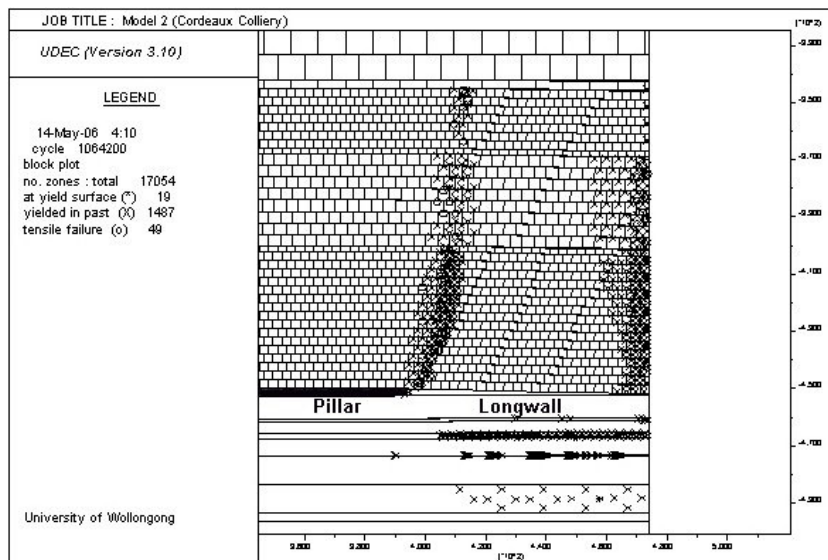


Fig. 4 - Typical cave zone above longwall panel

The analysed results from Models 1, 2 and 3 are shown below in Table 9.

Table 9 - Results

Parameter	Model 1	Model 2	Model 3
W (m)	105	158	160
H (m)	413	450	288
T (m)	2.7	2.5	3.0
W/H	0.25	0.35	0.56
$S_{max}$ (mm)	41.12	162.39	312.72
$S_{goaf}$ (mm)	39.64	82.64	87.24
+ $E_{max}$ (mm/m)	0.092	0.139	0.690
- $E_{max}$ (mm/m)	0.065	0.287	0.516
$G_{max}$ (mm/m)	0.086	1.275	3.731
D (m)	-96.00	5.50	18.50
$S_{max}/T$	0.015	0.065	0.104
$S_{goaf}/S_{max}$	0.964	0.509	0.279
K1	0.924	0.386	0.635
K2	0.653	0.794	0.475
K3	0.864	3.533	3.436
D/H	-0.232	0.012	0.064

To put the results into perspective, the results from Table 9 are reproduced on the corresponding empirical curves from Holla and Barclay (2000). These are shown below in Figures 5, 6, 7, 8, 9 and 10.

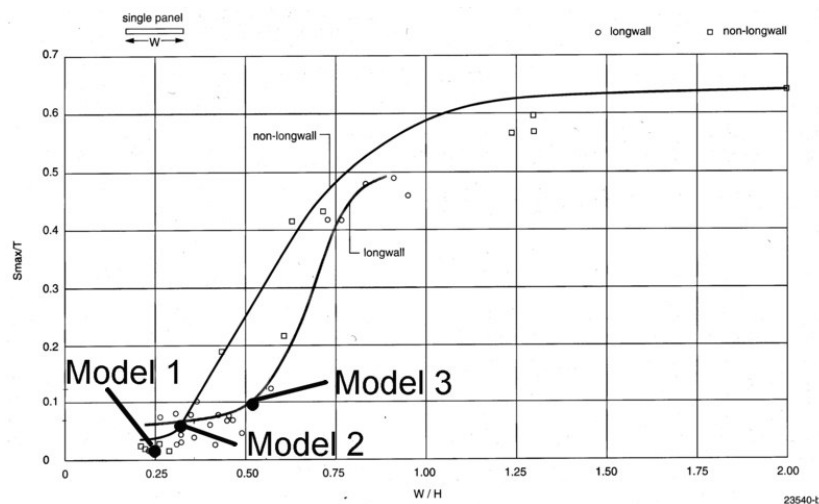


Fig. 5 - Model results for  $S_{max}/T$  (after Holla and Barclay, 2000)

It can be seen from Figures 5 and 6 that the numerical models predict maximum developed subsidence and goaf edge subsidence quite well. Given the amount of scatter in the empirical data for the subsidence values, this is a good result.

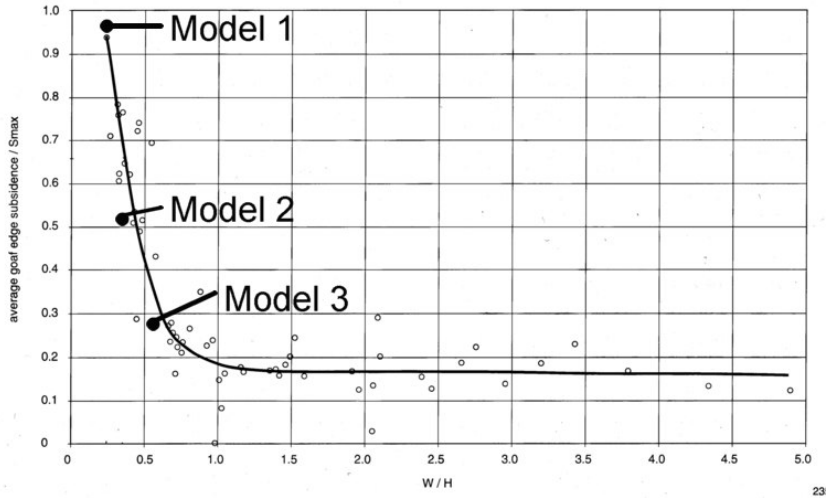


Fig. 6 - Model results for  $S_{goaf}/S_{max}$  (after Holla and Barclay, 2000)

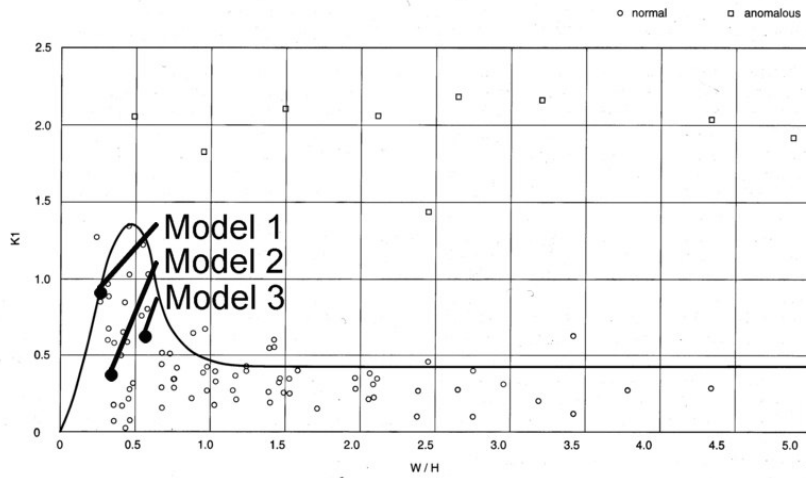


Fig. 7 - Model results for K1 (after Holla and Barclay, 2000)

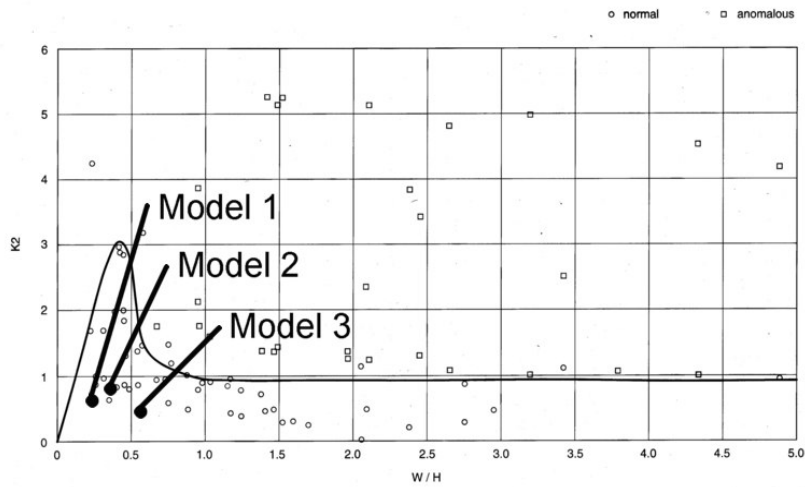


Fig. 8 - Model results for K2 (after Holla and Barclay, 2000)

Strain has been recognised as one of the most difficult parameters to predict due to vertical joints potentially opening up on the surface and the large effect that variations in topography has on the strain profile. Observed strain profiles in the field are never as perfect as theoretical strain profiles due to these factors.

It can be seen from Figures 7 and 8, the model results contain considerable scatter in the data points, as do the empirical results for the strain constants. Part of the problem is the use of the K1 and K2 constant which normalise strains to depth and  $S_{max}$  – this may not be valid for subcritical extraction.

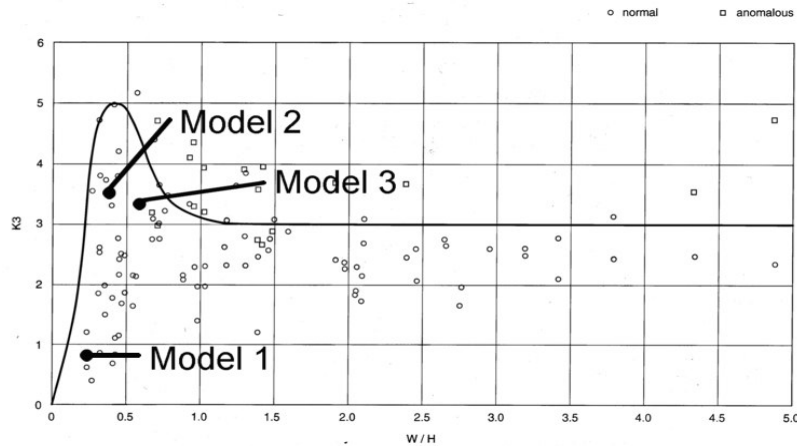


Fig. 9 - Model results for K3 (after Holla and Barclay, 2000)

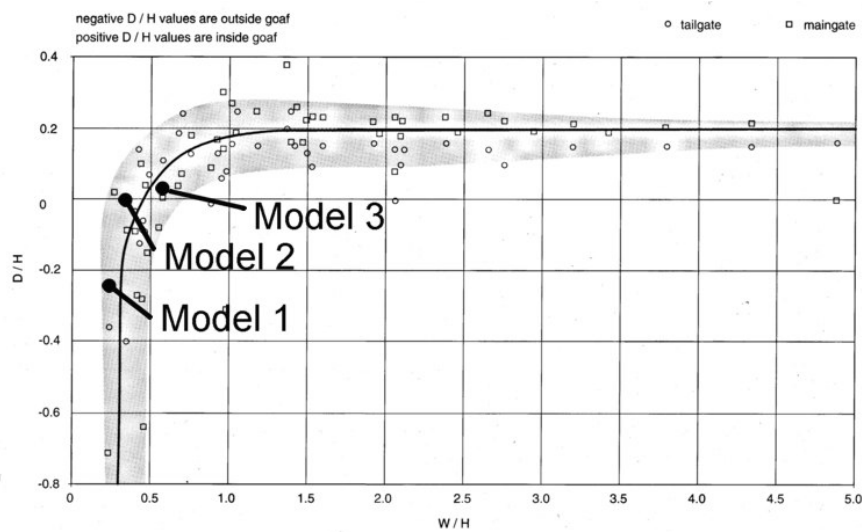


Fig. 10 - Model results for D/H (after Holla and Barclay, 2000)

The model results for tilt and its associated constant produced good matches with the empirical results. The model results for the tilt constant can be seen in Figure 9.

The results of the position of the inflection point relative to the goaf can be seen in Figure 10. It is noted by Holla and Barclay (2000) that the position of the inflection point falls inside the goaf for W/H ratios greater than 0.5 or outside the goaf for W/H ratios less than 0.5. It can be seen that this observation holds true for Model 1 (W/H = 0.25) and Model 3 (W/H = 0.56). The location of the inflection point is within 32 m of the position of maximum tilt for all three models. The subsidence at the inflection point is roughly one half of  $S_{max}$  for all models and this is in agreement with Holla and Barclay (2000).

The calculated angle of draw for the models varies between 19° and 41°. This produced an average value of 30°, which is very close to the average value of 29° stated by Holla and Barclay (2000).

---

## SUMMARY

Due to the ongoing nature of this project, the results presented are preliminary and are encouraging. The main aspects of subsidence development are represented generally well with the numerical modelling. It is anticipated that further verification can be achieved by the application of voussoir beam methods to the Bulgo Sandstone, as it appears to act as a massive elastic unit and the resulting subsidence should be primarily a function of the deflection of this unit.

The next step will be the construction of models that simulate undermined river valleys. These models will be ideally based on the models presented in this paper, and the location of the valley will be varied in its position relative to the centre of the longwall panel. It is anticipated that this modelling will shed some light on the mechanisms behind valley closure.

## ACKNOWLEDGMENTS

The authors wish to express their thanks to Seedsman Geotechnics Pty. Ltd. for financial support, BHP Illawarra Coal Pty. Ltd. for access to drill cores, and Strata Control Technology Operations Pty. Ltd. for their cooperation and helpful insights with core logging data and laboratory results. Thanks are also extended to Michael Coulthard of M.A Coulthard and Associates Pty. Ltd. for his technical guidance on the use of UDEC.

## REFERENCES

- ACARP, 2002. Management Information Handbook on the Undermining of Cliffs, Gorges and River Systems, ACARP Project No C8005 and C9067.
- Badelow, F, Best, R, Bertuzzi, R and Maconochie, D, 2005. Modelling of defect and rock bolt behaviour in geotechnical numerical analysis for Lane Cove Tunnel, in *Proceedings Geotechnical Aspects of Tunnelling for Infrastructure Projects, Mini-Symposium 12<sup>th</sup> October 2005, Milsons Point, Australia*, 9 p.
- Barton, N, 1976. The shear strength of rock and rock joints, *Int. J. Rock. Mech. Min. Sci. & Geomech. Abstr.* 13(10).
- Chan, K F, Kotze, G P and Stone, P C, 2005. Geotechnical modelling of station caverns for the Epping to Chatswood rail line project, in *Proceedings Geotechnical Aspects of Tunnelling for Infrastructure Projects, Mini-Symposium 12<sup>th</sup> October 2005, Milsons Point, Australia*, 15 p.
- Coulthard, M A, 1995. Distinct element modelling of mining-induced subsidence – A case study, in *Fractured and Jointed Rock Masses* (eds: Myer, Cook, Goodman and Tsang), 8 p (Balkema: Rotterdam).
- CSIRO Petroleum, 2002. Numerical Modelling Studies, in ACARP Project No C9067.
- CSIRO Exploration and Mining, 1999. Ground behaviour about longwall faces and its effect on mining, ACARP Project No C5017.
- Gale, W J, 2005. Application of computer modelling in the understanding of caving and induced hydraulic conductivity about longwall panels, in *Proceedings Coal2005 - 6<sup>th</sup> Australasian Coal Operators' Conference, 26-28 April 2005, Brisbane, Australia*. pp 11-15 (The Australasian Institute of Mining and Metallurgy: Melbourne).
- Ghobadi, M H, 1994. Engineering Geologic Factors Influencing the Stability of Slopes in the Northern Illawarra Region, PhD Thesis (unpublished), The University of Wollongong, Australia.
- Holla, L and Barclay, E, 2000. *Mine subsidence in the Southern Coalfield, NSW, Australia*, pp 1-16 (New South Wales Department of Mineral Resources).
- Itasca, 2000. *UDEC User's Guide*, (Itasca Consulting Group, Inc: Minneapolis, Minnesota, USA).
- Kapp, W A, 1984. Mine Subsidence and Strata Control in the Newcastle District of the Northern Coalfield New South Wales, PhD thesis (unpublished), University of Wollongong, Australia, pp 7, 8, 91.
- Kratzsch, H, 1983. *Mining Subsidence Engineering*, pp 41, 153 (Springer-Verlag).
- Mandl, G, 2005. *Rock Joints – The Mechanical Genesis*, pp 55-97 (Springer-Verlag: Germany).
- MacGregor, S and Conquest, G, 2005. Geotechnical characterization and borehole completion logs for surface boreholes: Endeavour 3 (WCC DDH29), Endeavour 4 (WCC DDH 30) and Endeavour 5 (WCC DDH 31), SCT Operations Pty Ltd, Rpt No BHPC2843.
- McNally, G H, 1996. Estimation of the geomechanical properties of coal measures rocks for numerical modelling, in *Proceedings Symposium on Geology in Longwall Mining, 12-13 November 1996*, (eds: McNally and Ward), pp 63-72.

- Pells, P J N, 1993. *The 1993 E.H Davis Memorial Lecture, Rock Mechanics and Engineering Geology in the Design of Underground Works*, pp 3.1-3.33 (Australian Geomechanics Society).
- Peng, S S, 1992. *Surface Subsidence Engineering*, Society for Mining, Metallurgy, and Exploration, Inc. (AIME), pp 1-20 (Braun-Brumfield, Inc.).
- Price, N J, 1966. *Fault and Joint Development in Brittle and Semi-Brittle Rock*, pp 144-147 (Pergamon Press Ltd: London).
- Seedsman, R W, 2004. Back analysis of sub-critical subsidence events in the Newcastle Coalfield using Voussoir beam concepts, in *Proceedings 6<sup>th</sup> Triennial Conference on Mine Subsidence (MTST), Maitland, NSW, Australia*, 9 p.
- Selley, R C, 2000. *Applied Sedimentology, Second Edition*, p 142 (Academic Press, California: USA).
- Tucker, M E, 2003. *Sedimentary Rocks in the Field, Third Edition*, pp 88-94 (John Wiley & Sons Ltd: England).
- Williams, W A and Gray, P A, 1980. The nature and properties of coal and coal measure strata, in *Proceedings Support in Coal Mines, The Aus. I.M.M., Illawarra Branch, Roof Support Colloquium, September, 1980*, (ed: A J Hargraves) pp 1-12.